To be presented at the Third Workshop on Structural Health Monitoring, Stanford, CA,
September 12-14, 2001

ARTIFICIAL NERVES FOR STRUCTURAL CONDITION MONITORING

William N. Martin Jr.[1], Anindya Ghoshal[1], Gary Lebbby[2], Mannur J. Sundaresan[1],
Mark J. Schulz[3], and Promod Pratap[4]

20011022 054

ABSTRACT

Structural condition monitoring refers to using in-situ sensors to monitor the internal loads and the health of a structure in real-time. This will allow a structure to be operated at its maximum performance and efficiency while minimizing the fatigue damage. To achieve this on a large structure, new highly distributed sensor concepts are investigated in which piezoceramic sensors are used to mimic biological nerves. A simulation model and a corresponding experiment show how these artificial nerves can measure large dynamic strains and simulated acoustic emissions that represent damage in structures.

INTRODUCTION

There is a need to develop techniques for in-situ real-time Structural Health Monitoring (SHM) that have high sensitivity and low cost for application to large structures and structures that have complex geometry. The complex geometry includes joints, ribs, varying thickness, curvature, fasteners, hybrid materials, and materials that are highly damped such as honeycomb sandwich structures. The difficulties of applying some of the more established techniques for damage detection to large structures are briefly discussed here. This background provides the impetus for the development of a technique that uses artificial nerves for structural condition monitoring, which is the focus of this paper.

The first approach considered uses active propagation of Lamb waves in the plane of the material to detect damage. The wave propagation method can detect damage accurately in structures by wave reflections from defects [1], or by transmitting and receiving waves and casting shadows [2]. However, for some applications the wave propagation approaches can become complex because many

[1]Department of Mechanical Engineering, [2]Department of Electrical Engineering, North Carolina A&T State University, Greensboro, NC 27411, [3]Department of Mechanical Engineering, University of Cincinnati, Cincinnati, OH 45221, [4]Department of Physics and Astronomy, University of North Carolina at Greensboro, Greensboro, NC 27402

sensor/actuator elements are required. The associated wiring, instrumentation, amplification, multiplexing, and computational resources required to implement these methods on a large scale can be prohibitive in terms of cost, added weight, and reliability.

Another possible approach for SHM is to monitor Acoustic Emissions (AE) caused by damage growth [3]. AE methods are passive and have been used in critical areas of aircraft and other structures in a few exploratory studies and have been effective in detecting small cracks in the neighborhood of the sensor. However, application of the conventional AE technique to SHM has been limited in practice. This is because it is impractical to embed or incorporate on the structure a large number of conventional AE sensors and signal processing channels, and because the AE waveforms that travel any significant distance are too complicated for purposes of source characterization.

A third approach for SHM is to monitor strains [4] over the structure. An active approach uses light waves and optical fibers with Bragg gratings to provide a localized strain measurement at each grating. This means that critical points can be monitored very accurately, but a large number of fibers and gratings would be required to monitor large or complex structures to detect small damage. The structure with the optical connections, multiplexer, and optical analyzer may become complex and expensive.

Trying to overcome the limitations of these techniques, another approach for SHM is to build an Artificial Neural System [5]. The artificial neural system uses piezoceramic elements to measure both acoustic emissions and dynamic strains. It is a passive technique that has a high sensor density to detect small defects and it simplifies the signal processing and instrumentation by mimicking the signal processing functions of biological systems. Besides health monitoring, the neural system can be used for Structural Condition Monitoring (SCM). SCM goes beyond SHM because it also provides dynamic strain and loads information that can be used to regulate loading in the structure to allow maximum efficiency to be achieved without damaging the structure due to fatigue or overload. The present limitations of the artificial neural system method are that the signal processing is more complex, and damage is not localized as well. Development of the artificial nerves for use in the artificial neural system is discussed in this paper.

Series and array configurations of the sensor nodes are being investigated [6-7] to build structural nerves. Piezoelectric patches are used as the sensor nodes. The sensor array mimics receptors that excite dendrites that are the inputs of neurons in the human nervous system. Ten or more nodes can be connected in a continuous single channel nerve. This continuous sensor approach is investigated first in the paper. Then, the same sensor elements used for the continuous sensor are connected in an N-by-N array that causes the individual signals from the sensors to be combined into 2N-1 array outputs, as compared to the single output from before. For large array sizes, this approach tremendously reduces the number of channels of data acquisition instrumentation needed for structural health monitoring. A trade-off in these two approaches is that the continuous sensor is the simplest with only one channel of data acquisition, while the array uses more channels to more accurately locate damage. The biological nerves are shown in Figure 1(a), a concept for four continuous nerve sensors connected together is shown in Figure 1(b), and an array

of four continuous nerve sensors is shown in Figure 1(c). In Figure 1(b,c), the small rectangles represent sensor nodes connected serially and the center element is the junction to that surrounding continuous sensor.
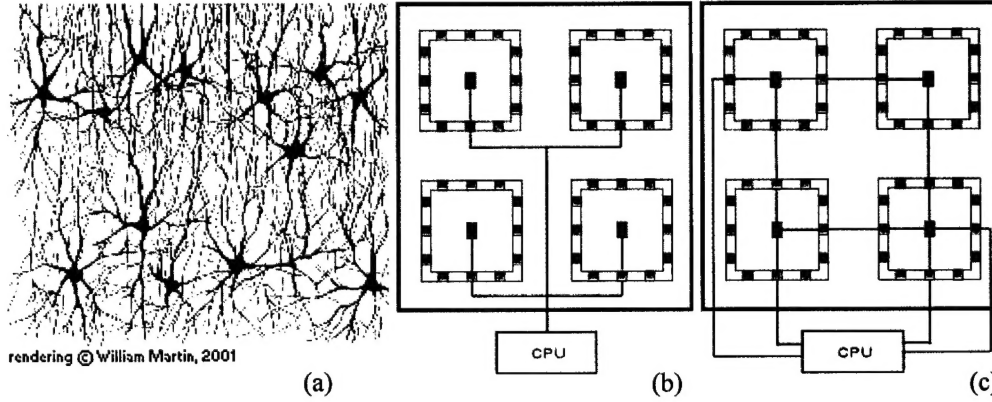
Figure 1. Neurons; (a) biological, (b) structural with four continuous sensors/receptors, (c) structural with hierarchical array sensors/receptors.

## MODELING AND TESTING OF THE CONTINUOUS NERVE

The electrical modeling of the nerves and a wave propagation model of a panel are discussed next. Because of the piezoelectric properties, the nodes can be modeled as a capacitor in parallel with a current source. The piezoelectric constitutive equations are listed in the IEEE standard ANSI/IEEE Std. 176-1987. These equations can be put into matrix form to give the piezoelectric constitutive equations:

$$\begin{bmatrix} D \\ T \end{bmatrix} = \begin{bmatrix} \varepsilon^S & e \\ -e_t & c^E \end{bmatrix} \cdot \begin{bmatrix} E \\ S \end{bmatrix}, \quad \begin{bmatrix} D \\ S \end{bmatrix} = \begin{bmatrix} \varepsilon^T & d \\ d_t & s^E \end{bmatrix} \cdot \begin{bmatrix} E \\ T \end{bmatrix}. \tag{1, 2}$$

The piezoceramic nerve shown in Figure 1(b) (one square) can be modeled using the piezoceramic constitutive equations and by connecting the segments into an electric circuit as shown in Fig. 2. Please refer to [8] for the full derivation, but the expression for the output voltage equation for a nerve is:

$$\frac{d}{dt}(i) + \frac{n \cdot i}{RC} = \frac{eA_e}{RC} \sum_{j=1}^{n} \dot{S}_j \tag{3}$$

where C is the capacitance of the AFC sensor, with an effective capacitor area of A_e, and effective plate separation distance h, i_c represents the component of the current going through the capacitor of the model, and i_g represents the component of the current generated by the piezoelectric fibers.
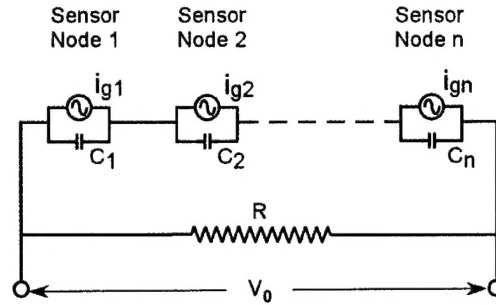
Figure 2. Circuit model of a nerve with nodes 1,2,…,n connected in series.

The homogeneous and particular solutions for Equation (3) must be calculated and added for the total solution of the current i. The product of the current $i(t)$, and the impedance R of the measuring device equals the voltage of the series connected sensors as a function of time. Thus we solve for the current to get the voltage $V_0 = iR$. This voltage is proportional to the dynamic strain in the structure at the sensor and thus can be used to detect damage through dynamic strain measurements and acoustic emissions. Because the term on the right hand side of Equation (3) depends on the strains imposed upon each sensor node in the series, it is difficult to get a closed form solution for the current. Thus, a Newmark-Beta explicit integration method is used to solve for the current in the simulation.

The key result of this analysis is contained in Equation (3). To obtain the maximum sensitivity from the continuous sensor we must make the right hand side of Equation (3) as large as possible. Because the strain levels in the structure are produced by high strains near the damage or by acoustic emissions from damage, the sensor should be as close as possible to the damage. This is a key advantage of using the artificial neural system; it can be distributed over the full structure. The sensor parameters in this equation must also be optimized. The resistance value in the circuit is the combination of the resistance of the electroding and the impedance of the measuring instrument. The resistance of the electroding must be minimized. The capacitance of the nerve is minimized by the series connectivity of the nodes. For series connectivity, the capacitance adds as the sums of reciprocals and therefore reduces the overall capacitance, but the resistances in series add directly. This analysis illustrates the advantage of the series sensor design and that the resistance of the nerve nodes must be small. This model of the nerve is very similar to the electrical model of the nerve cell [9]. The artificial nerve is similar in behavior and modeling to the nerve cell, but the stimulus is by electro-chemical processes in the biological cell and by piezoelectric processes in the structural material. This analysis has modeled the linear nerve. The active and nonlinear functions of nerve cells are also important, but are not discussed here.

Certain assumptions are made when calculating the output current of the series circuit. These are; (1) The storage capacities of the piezoelectric sensors are not breached during excitation, and each sensor is being excited below its resonance frequency; (2) The structure to which the sensors are bonded has significantly higher inertia and stiffness compared to the sensors, so that the structural strain field is unaffected by the converse piezoelectric effect caused by sensor excitation; and

(3) The dielectric element of the piezoelectric sensor is ideal; meaning that no leakage of current exists in the dielectric of the capacitive element of the sensor. With these assumptions, we can model the sensor as a capacitor in parallel with a current source because a perfect capacitor would have an "infinite"-resistance and act as an open circuit.

We have discussed the electrical modeling and this model must be connected to a structural model to simulate the behavior of the neural system. We have developed an algorithm to study the benefits of the neural sensor. The algorithm computes the response of the nerve caused by acoustic waves propagating in a plate. The algorithm uses the physical parameters of the nerve, the piezoelectric constitutive equation, and a step input to a plate, and it computes the voltage as the wave passes over the sensor nodes of the nerve. The code takes into account (integrates) the exact strains over the area of the sensor node to compute the voltage output. Details of the plate model are given in [8]. The panel modeled and used for experimentation is shown in Figure 3. A special fixture shown in Figure 3 was built to model a simply supported boundary condition because this is the easiest boundary condition from which a closed for solution to the plate equation is possible. Testing was performed and the simulation and test results are compared in the following section.

The simulation is performed using a model of the fiberglass plate shown in Figure 3. Nine small piezoceramic patches are modeled connected in series to form a continuous nerve. A step function input of 1 Newton is put near the center of the panel to model an acoustic emission that would occur from a crack in the panel. The scaled initial response of the panel is shown in Figure 4. The simulation amplitude shown was scaled (reduced) by a factor of 7.5 to more closely match the magnitude of test results. It is thought that the test setup may have resistance and capacitance in the wiring not modeled in the simulation. Since the charge produced by the sensor is small, the added resistance could have a significant effect on the voltage output. No amplifier is used in this experiment. Also, the first natural frequency for the plate in the simulation is 10.8Hz, while the first frequency for the actual test panel is 17Hz. The first natural frequency for a plate for the fixed boundary condition is 21Hz. The boundary condition for the test panel is thus apparently closer to fixed than free. This stiffer boundary may also have caused the test response to be smaller than the simulation.

The panel in Figure 3 is used for the testing. A 0.3mm pencil lead is used to simulate an acoustic emission near the center of the panel. The test response of the single channel continuous sensor is shown in Figure 4. The peak voltage for the test is 0.1V and it occurs at about 0.6 milliseconds after the impulse starts. The responses of the simulation and test have approximately the same character. The simulation models asymmetric waves only, while the test has some contribution from symmetric Lamb waves that causes some of the difference in the two responses. However, the simulation models the main characteristics of the response of sensor and panel reasonably well. The lead break was done repeatedly at the same location and the waveforms are quite repeatable.
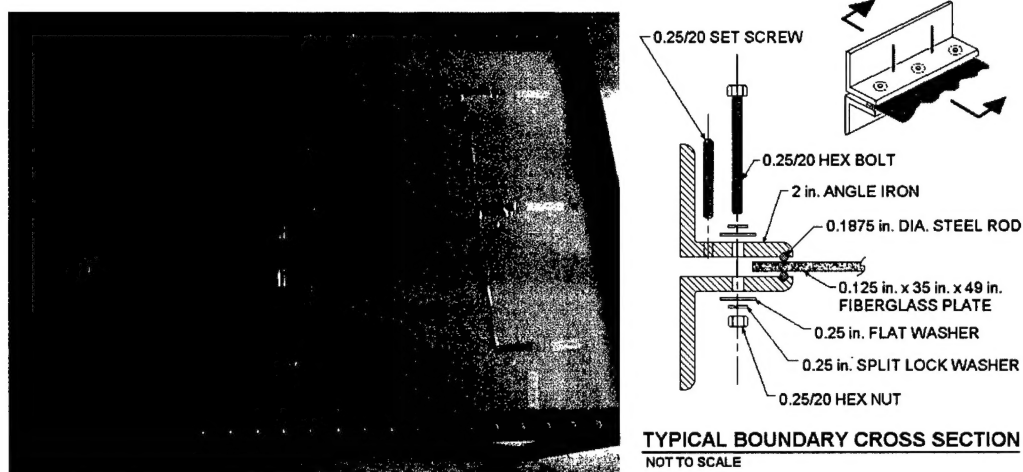
Figure 3. A fiberglass panel with a neural sensor, and detail of the boundary.
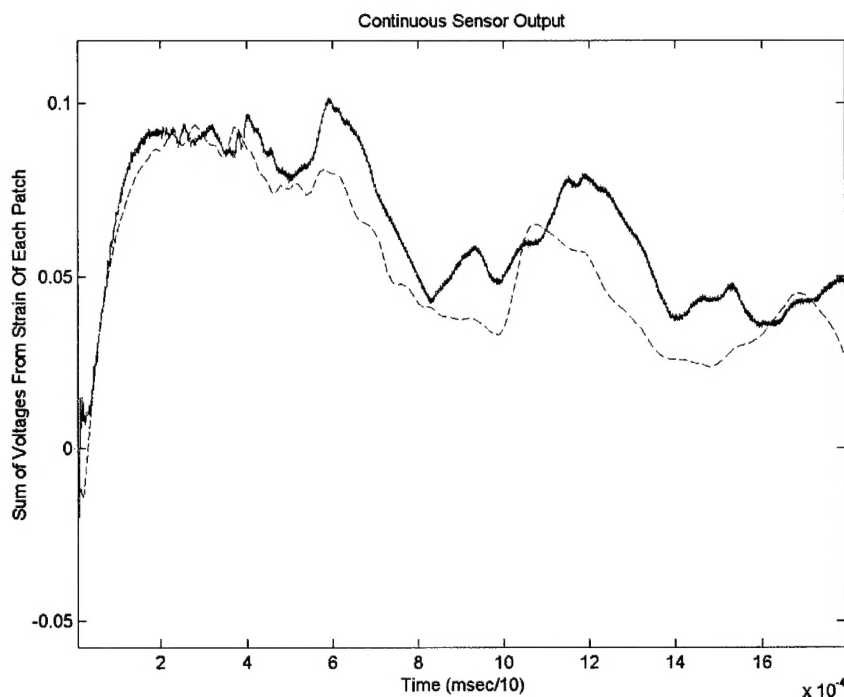
Figure 4. Voltage response of the continuous nerve due to a 0.3 mm lead break. Scaled simulation result (dashed) shown with experiment result (solid).

The lead break was also done near the edge of the plate and the simulation and test responses also compared reasonably well, except the simulation result was always greater then the test by about the factor of 7.5. Modeling the resistance and capacitance of the wiring and reducing the clamping force on the boundary are to be done in further experimentation and are expected to bring the simulation and test amplitudes closer together.

MODELING AND TESTING OF THE ARRAY NERVE

The plate with the nine sensor nodes used in the simulation and experiment just discussed are used again, but the sensor nodes are connected in a cross-array pattern now with three rows and three columns. This gives 2N-1=5 channels of voltage output where one channel is used for a ground connection. The connectivity of the array is shown in Figure 5. The electrical modeling of the array was done using the piezoelectric constitutive equations and writing Kirchhoff's voltage and current equations for the circuit.
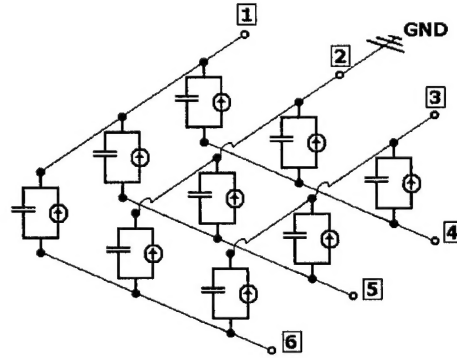

Figure 5. Cross-sensor nerve array with nine piezoceramic nodes.

The equations modeling the strain and open circuit voltage response of the array derived using (1-3) and Kirchhoff's current and voltage laws and are:

$$\dot{v} = \alpha W \dot{s} + \beta M v \qquad (4)$$

where $\dot{v}$ is a vector representing the voltage rate at each sensor node, v represents the voltage at each sensor node, $\dot{s}$ is the strain rate vector, $\alpha = -eA_e/(27 \cdot C)$, where e is the induced stress constant, A_e is the area of the electroding, and C is the capacitance of one node, and $\beta = 1/(81 \cdot R \cdot C)$, where R is the of the measuring device. The matrices W, T, and M are defined as follows:

$$
W = \begin{bmatrix}
15 & 6 & 6 & 6 & -3 & -3 & 6 & -3 & -3 \\
6 & 15 & 6 & -3 & 6 & -3 & -3 & 6 & -3 \\
7 & 4 & 16 & -2 & -5 & 7 & -5 & -8 & 4 \\
6 & -3 & -3 & 15 & 6 & 6 & 6 & -3 & -3 \\
-3 & 6 & -3 & 6 & 15 & 6 & -3 & 6 & -3 \\
-2 & -5 & 7 & 7 & 4 & 16 & -5 & -8 & 4 \\
6 & -3 & -3 & 6 & -3 & -3 & 15 & 6 & 6 \\
-3 & 6 & -3 & -3 & 6 & -3 & 6 & 15 & 6 \\
-2 & -5 & 7 & -2 & -5 & 7 & 4 & 1 & 13
\end{bmatrix}; \quad
\dot{v} = \begin{bmatrix}
\dot{v}_{11} \\ \dot{v}_{12} \\ \dot{v}_{13} \\ \dot{v}_{21} \\ \dot{v}_{22} \\ \dot{v}_{23} \\ \dot{v}_{31} \\ \dot{v}_{32} \\ \dot{v}_{33}
\end{bmatrix}; \quad
T = \begin{bmatrix}
1 & 0 & 0 & -1 & 0 \\
1 & 0 & 0 & 0 & 0 \\
1 & 0 & 0 & 0 & -1 \\
0 & 1 & 0 & -1 & 0 \\
0 & 1 & 0 & 0 & 0 \\
0 & 1 & 0 & 0 & -1 \\
0 & 0 & 1 & -1 & 0 \\
0 & 0 & 1 & 0 & 0 \\
0 & 0 & 1 & 0 & -1
\end{bmatrix}
\qquad (5,6)
$$

$$M = \begin{bmatrix} 21 & -15 & 12 & 3 & -6 & -6 & 3 & -6 & -6 \\ 3 & 39 & 3 & -15 & 48 & -15 & -15 & 39 & -15 \\ 17 & -31 & 26 & -1 & -22 & 8 & -7 & -7 & 2 \\ 3 & -6 & -6 & 21 & -15 & 12 & 3 & -6 & -6 \\ -15 & 48 & -15 & 3 & 39 & 3 & -15 & 39 & -15 \\ -1 & -22 & 8 & 17 & -31 & 26 & -7 & -7 & 2 \\ 3 & -6 & -6 & 3 & -6 & -6 & 21 & -15 & 12 \\ -15 & 48 & -15 & -15 & 48 & -15 & 3 & 30 & 3 \\ -1 & -22 & 8 & -1 & -22 & 8 & 11 & -16 & 20 \end{bmatrix}; \quad \dot{s} = \begin{bmatrix} \dot{s}_{11} \\ \dot{s}_{12} \\ \dot{s}_{13} \\ \dot{s}_{21} \\ \dot{s}_{22} \\ \dot{s}_{23} \\ \dot{s}_{31} \\ \dot{s}_{32} \\ \dot{s}_{33} \end{bmatrix} \quad (7)$$

The voltage, v, is proportional to the dynamic strain in the structure at the sensor interfaces (similar to the continuous sensor) and thus can be used to detect damage through dynamic strain measurements and acoustic emissions. Since Equation (4) depends on the voltages and voltage rates at each sensor node in the series, it is difficult to get a closed form solution for the array voltages. Thus, a Newmark-Beta explicit integration method is used to solve for the voltage in the simulation.

The rank of matrix W is five, thus the rank of M is also five therefore, they cannot be inverted. This means that the strains at the nine nodes cannot be uniquely determined by measuring the six voltages of the array and then computing the nine voltages of the nodes. There is a trade-off of the array design of Fig. 5; the voltage field over the array can be measured, but the voltages at each node depend on the local strain field and the strain field over the entire array. Here T, in Equation (6) is the transformation matrix between the voltages at the nodes and at the five array output wires in Figure 5, with the j=2 connection used as the ground. Equation (6) allows voltages at the nine nodes to be computed exactly from the known voltages at the five array output wires. Looking at the values in the W matrix shows the largest values are on the diagonals. This indicates that the voltage output at a node is due to strain at that node plus smaller contributions from any initial voltages at other nodes. The voltage rates across each sensor node are given by (4).

The solution of (4) to obtain the approximate strain field is being done using a neural network method and is not reported here. The advantage of the technique is that the number of wire connections needed is 2N for a square array, while the voltages at NxN sensor nodes can be determined by multiplexing using two channels of data acquisition, or using 2N-1 channels of data acquisition simultaneously. The simulation and test responses of the five array outputs are shown in Figure 6 as a result of a lead break near the center of the panel. The simulation response was again reduced by a factor of 7.5 amplitude to match the test amplitudes. The characteristics of the responses for the simulation and test are similar. The peak voltage in the simulation is 0.065V and it occurs at 11.5 milliseconds. The peak voltage in the test is 0.045V and it occurs at 11 milliseconds.
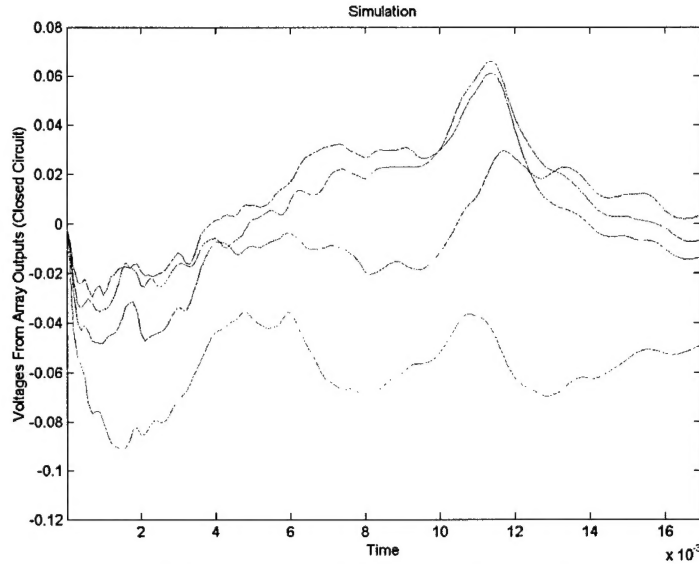
Figure 6a. Simulation scaled response of the neural array due to center excitation.
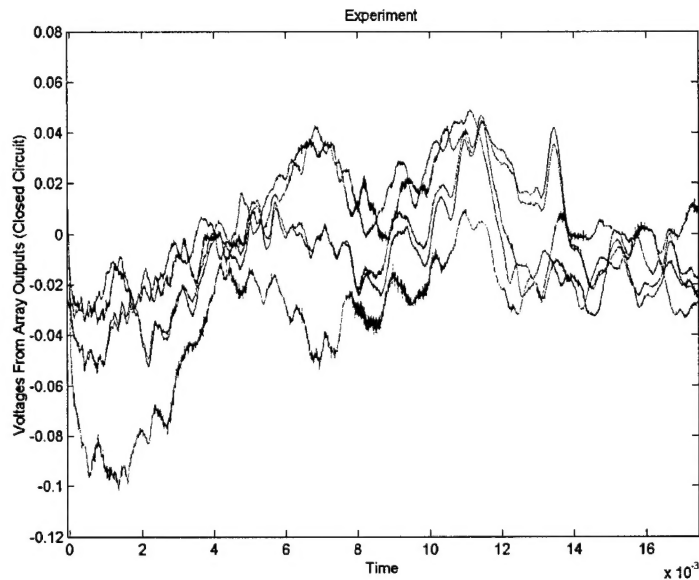
Figure 6b. Response of the neural array due to center excitation (Test result).

CONCLUSIONS

The simulation and testing performed have shown that multiple piezoceramic patches can be connected together in a series or array pattern to simulate the way biological nerves have multiple inputs (dendrites) connected together. This reduces the number of channels of data acquisition needed to detect damage represented by acoustic emissions or high strains. The form of the response of the test and simulation responses obtained were similar, but the simulation predicted larger voltages than the test. More detailed modeling of the electrical circuit and boundary

conditions are expected to bring the amplitudes of the simulation closer to the test response. Ambient noise and filtering are other factors in the design not discussed in this paper. The nerves discussed in this paper are components in an artificial neural system that is expected to provide a simple method of condition monitoring for large and complex structures. The simulation model developed can be used to optimize the design of the neural system for different structural materials and sizes.

ACKNOWLEDGMENT

REFERENCES

1. Wang, C., Chang, F., "Diagnosis of Impact Damage in Composite Structures with Built-In Piezoelectrics Network," *Proceedings of the SPIE*, Vol. 3990, p. 13, 2000.
2. Schwartz, W.G., Read, M.E., Kremer, M.J., Hinders, M.K., Smith, B.T., "Lamb Wave Tomographic Imaging System for Aircraft Structural Health Assessment," *SPIE Conference on NDE of Aging Aircraft, Airports, and Aerospace Hardware III*, Vol. 3586, P. 292, 1999, Newport Beach, CA.
3. Searle, I., Ziola, S., May, S., "Damage Detection Experiments and Analysis for the F-16," *Proceedings of the International Workshop on Structural Health Monitoring*, Stanford University, Stanford, CA., September 18-20, 1997, p. 310-324.
4. Kim, K.S., Paik, S.H., Optical Fiber Monitoring System of Bridges in Korea, *Proceedings of the International Workshop on Structural Health Monitoring*, Stanford University, Stanford, CA., September 18-20, 1997, p. 555-563.
5. Sundaresan, M.J., Schulz, M.J., Ghoshal, A., Pratap, P., "A Neural System for Structural Health Monitoring," *SPIE 8th Int. Symposium on Smart Materials and Structures*, March 4-8, 2001.
6. Sundaresan, M.J., Ghoshal, A., and Schulz, M.J., "Sensor Array System," patent application, 6/00.
7. Ghoshal, A., Sundaresan, M.J., Schulz, M.J., Pai, P.F., "Continuous Sensors for Structural Health Monitoring," Adaptive Structures and Material Systems Symposium at the International Mechanical Engineering Congress and Exposition Winter Annual Meeting of the ASME, Nov. 5-10, 2000, Walt Disney World Dolphin, Orlando, Fla.
8. Schulz, M. J. Sundaresan, M.J., Ghoshal, A., Martin, W.N., "Evaluation of Distributed Sensors for Structural Health Monitoring," *ASME DTEC'01 Conf.*, Sept. 9-12, Pittsburgh, PA, 2001.
9. Zigmond, M.J., Boom, F., Landis, S.C., Roberts, J.L., Squire, L.R., Fundamental Neuroscience, *Academic Press*.